RSC Advances

PAPER

View Article Online
View Journal | View Issue

Cite this: *RSC Adv.*, 2019, **9**, 2746

Developing a CO_2 bicarbonation absorber for promoting microalgal growth rates with an improved photosynthesis pathway

Wangbiao Guo,[a] Jun Cheng,*[a] Yanmei Song,[a] Santosh Kumar,[a] Kubar Ameer Ali,[a] Caifeng Guo[b] and Zhanshan Qiao[b]

Received 20th November 2018
Accepted 2nd January 2019

DOI: 10.1039/c8ra09538h

rsc.li/rsc-advances

In order to solve the problems of the short residence time and low utilization efficiency of carbon dioxide (CO_2) gas added directly to a raceway pond, a CO_2 bicarbonation absorber (CBA) was proposed to efficiently convert CO_2 gas and sodium carbonate (Na_2CO_3) solution to sodium bicarbonate ($NaHCO_3$), which was dissolved easily in the culture medium and left to promote the microalgal growth rate. The CO_2 gas reacted with the Na_2CO_3 solution (initial concentration = 200 mM L^{-1} and volume ratio in CBA = 60%) for 90 min at 0.3 MPa to give the optimized molar proportion (92%) of $NaHCO_3$ product in total inorganic carbon and increase the microalgal growth rate by 5.0 times. Quantitative label-free protein analysis showed that the expression levels of the photosystem II (PSII) reaction centre protein (*PsbH*) and PSII cytochrome (*PsbV2*) in the photosynthesis pathway increased by 4.8 and 3.4 times, respectively, while that of the RuBisCO enzyme (*rbcL*) in the carbon fixation pathway increased by 3.5 times in *Arthrospira platensis* cells cultivated with the $NaHCO_3$ product in the CBA at 0.3 MPa.

1. Introduction

Cultivating microalgal for the carbon dioxide (CO_2) fixation from coal-fired power plants has been extensively studied in the past few decades. Normally, 1 ton of microalgal can consume 1.83 tons of CO_2 with a carbon content of 50% in the microalgal cells. It was reported that around one-third of global CO_2 fixation was attributed to the microalgal.[1,2] The reason for this is because there is a CO_2-concentrating mechanism (CCM) in the pyrenoid organelle of the algal cell that accelerates CO_2 assimilation.[3,4] According to the CCM, the HCO_3^- passes successively through the plasma membrane, the chloroplast envelope and the thylakoid membrane and this is mediated by the enzyme, carbonic anhydrase (CA). Then when the HCO_3^- reaches the thylakoid lumen, it is catalysed to CO_2. Finally, the CO_2 is fixed by ribulose-1,5-biphosphate carboxylase/oxygenase (RuBisCO) and channelled into the Calvin cycle.[1,2] The HCO_3^- is therefore the dominant type of carbon to be absorbed for photosynthesis in microalgal cells.

Normally, the CO_2 gas is added directly into the microalgal solution by using an aerator.[5–9] Researchers have proposed several aerators[10–12] and baffles[13–18] for use in the raceway pond (RWP) to increase the CO_2 bubble residence time for improving the conversion efficiency of CO_2 to HCO_3^- ($CO_2 + CO_3^{2-} + H_2O \rightarrow 2HCO_3^-$). However, the reaction of CO_2 and CO_3^{2-} requires relatively high pressure and sufficient reaction time.[19,20] Because the bubble residence time is relatively low (usually several seconds) when the CO_2 gas is added directly by the aerator[21,22] at atmospheric pressure, and was harmful to the reaction of CO_2 and CO_3^{2-}, most of the CO_2 bubbles were emitted to the atmosphere again, causing wastage and low CO_2 utilization efficiency. It is also not beneficial for microalgal growth rate.

The CO_2 bicarbonation absorber (CBA) has been generally adopted to produce sodium bicarbonate ($NaHCO_3$) in industry.[23–26] A gas distributor was needed on the bottom of the CBA to provide a uniform gas flow distribution. The CO_2 gas was added to the CBA from the bottom inlet hole, while the sodium carbonate mixture flowed in from the top of the CBA. The reaction pressure and temperature were strictly controlled to produce ($NaHCO_3$) crystals at the end of the reaction. On the basis of this technology, the CBA could be combined with the RWP so that the CO_2 gas can be converted to HCO_3^- more efficiently, because the CO_2 molecule was reacted with the HCO_3^- in advance, which made it easier for the algal cell to absorb it. However, the CBA could not be applied to the RWP, because the HCO_3^- concentration was fairly high, and even crystallized. Because the algal cells only required a limited HCO_3^- concentration, a higher HCO_3^- concentration would cause a drop in pH levels and the proton gradient. Zhang *et al.*[27] proposed a spraying absorption tower coupled with an outdoor open RWP based on this principle to improve the CO_2 utilization efficiency. The pH value was controlled by the absorption

[a]State Key Laboratory of Clean Energy Utilization, Zhejiang University, Hangzhou 310027, China. E-mail: juncheng@zju.edu.cn; Fax: +86 571 87951616; Tel: +86 571 87952889

[b]Ordos Jiali Spirulina Co., Ltd, Ordos 016199, China

tower. The biomass productivity increased by 40.7% and CO_2 fixation efficiency reached 50% compared to the conventional process where the CO_2 was added through porous pipes placed at the bottom of the RWP.[27] However, the use of the proposed spraying absorption tower did not take into account the CO_2 exhaust gas, which was emitted directly to the atmosphere, causing a secondary emission of CO_2 gas. Also, the optimized operation parameters were not given in this study. Eloka-Eboka and Inambao[28] investigated the rate of sequestration of both total and dissolved carbon, and suggested that *Dunaliella* has a higher CO_2 uptake rate. However, they did not give the specific method for improving the CO_2 uptake rate in a real application, and the relationship of HCO_3^- concentration and biomass growth rate was not studied. Mokashi *et al.*[29] also proved that HCO_3^- can be an alternative inorganic carbon source for higher microalgal production. Therefore, it is necessary to develop an apparatus to convert CO_2 to HCO_3^- efficiently. The CO_2 fixation efficiency would improve considerably if CO_2 was reacted to HCO_3^- and fixed by the algal cell.

The main purpose of this study was to find an efficient method for CO_2 fixation by microalgal. A CBA was proposed which would convert the CO_2 gas to HCO_3^-, which can be easily utilized by the microalgal cells and dramatically enhances the CO_2 fixation efficiency. The exhausted CO_2 gas was recycled to the inlet gas flow, which means that the CO_2 gas was completely reacted to the HCO_3^-, so CO_2 fixation efficiency was greatly enhanced. The reaction time and pressure were optimized to regulate the molar proportion of $NaHCO_3$ in total inorganic carbon. The initial concentration of sodium carbonate (Na_2CO_3) in the substrate and the volume ratio of Na_2CO_3 solution in the CBA were optimized to regulate the $NaHCO_3$ product and to improve the biomass growth rate. Furthermore, the metabolism pathway of photosynthesis and CO_2 fixation were determined to further understand the absorption mechanism of HCO_3^- by the algal cell.

2. Materials and methods

2.1 Design of CO_2 bicarbonation absorber

As shown in Fig. 1, a CBA was proposed for improving the microalgal growth rate. The CBA was made of plexiglass, which gives a maximum CO_2 pressure of 1.0 MPa. The dimensions of the CBA were $\varnothing 5 \times 70$ cm. The CBA was used for the reaction of CO_2 and Na_2CO_3 ($Na_2CO_3 + CO_2 + H_2O \rightarrow 2NaHCO_3$). During the reaction, the CO_2 gas in the storage tank was dried by a drier and then flowed into the CBA. A check valve was installed before the CO_2 inlet to prevent the backward flow of gas. A pressure valve was installed before the check valve to keep the reaction pressure within 0.1 to 0.5 MPa. Simultaneously, the Na_2CO_3 was dissolved in water and injected to the CBA using a pump with the Na_2CO_3 concentration ranging from 120 to 280 mM L^{-1}. The initial volume ratio μ of the Na_2CO_3 solution in CBA was defined as the ratio of solution height h_1 and reactor height h_2, that is, $\mu = h_1/h_2$. In order to improve the CO_2 utilization efficiency, the exhaust CO_2 gas was dried and returned back into the CBA. For a better distribution of CO_2 gas in the CBA, there was a cavity on the bottom of the reactor, above which was a gas distributor. The gas distributor was comprised of several holes which increased the CO_2 resistance time and improved the reaction efficiency of CO_2 and Na_2CO_3. The reaction time varied from 30 to 150 min. After the reaction, the solution mixture flowed into the RWP for the cultivation of microalgal.

2.2 Cultivation of *Arthrospira platensis*

The algal strain *Arthrospira* was mutated using nuclear irradiation and domestication in a high CO_2 concentration environment[30] to obtain hereditary stability. As well as the solution mixture of $NaHCO_3$ and Na_2CO_3 from CBA, the culture medium was composed of 2.5 g L^{-1} sodium nitrate ($NaNO_3$), 0.5 g L^{-1} dipotassium phosphate (K_2HPO_4), 0.2 g L^{-1} magnesium sulfate heptahydrate ($MgSO_4 \cdot 7H_2O$), 1.0 g L^{-1} potassium sulfate (K_2SO_4), 0.01 g L^{-1} ferrous sulfate heptahydrate ($FeSO_4 \cdot 7H_2O$), 0.08 g L^{-1} disodium ethylenediaminetetraacetate dihydrate (Na_2EDTA), 0.04 g L^{-1} calcium chloride ($CaCl_2$), 3 mL hydrochloric acid (HCl) (35% w/v) and 1 mL A_5. A_5 refers to the micronutrients required for the growth of the microalgal, including 2.86 g L^{-1} boric acid (H_3BO_3), 1.81 g L^{-1} manganese(II) chloride tetrahydrate ($MnCl_2 \cdot 4H_2O$), 0.22 g L^{-1} zinc sulfate heptahydrate ($ZnSO_4 \cdot 7H_2O$), 0.08 g L^{-1} copper(II) hydrate pentahydrate ($CuSO_4 \cdot 5H_2O$) and 0.01 g L^{-1} molybdenum trihydrate (MoO_3). The algal were inoculated into RWP with a solution depth of 5 cm and absorbance value of 0.3. The dimension of the RWP was $20 \times 8 \times 5$ cm. The solution temperature was kept at 30 ± 2 °C and light intensity on the surface of the RWP was 8000 ± 500 lux. The RWP was covered with a plastic membrane to prevent evaporation of the microalgal solution. During the experiments, the algal samples were collected at 9 : 00 and 21 : 00 every day, and the solution optical density (OD) and pH were measured. The curve fitting of the OD and cell density (C) was measured as C (g L^{-1}) = $0.505 \times OD_{560nm} - 0.034$ ($R^2 = 0.996$). All the experiments were conducted in triplicate. The solution concentration of total inorganic carbon (TIC), $NaHCO_3$ and Na_2CO_3 were measured using a double-tracer method.[31–34]

2.3 Quantitative label-free protein measurement

The direct mass spectrometry analysis of protein peptide segments was conducted using a label-free method.[35] It was effective and efficient for quantitatively determining the protein functions. The label-free method mainly included three steps:[36,37]

2.3.1 Total protein extraction. The sample was milled to a powder in a mortar with liquid nitrogen followed by mixing 150 mg of the powder from each sample with 1 mL of lysis buffer [2-amino-2-(hydroxymethyl)-1,3-propanediol, TRIS base, pH 8], 8 M urea and 1% sodium dodecyl sulfate with protease inhibitor cocktail in a glass homogenizer. After homogenization, the homogenate was incubated on ice for 20 min and centrifuged at 12 000 × g for 15 min at 4 °C. The supernatant was transferred to a clean tube, and the protein concentration was determined using the Bradford assay. To the supernatant, 4 volumes of 10 mM dithiothreitol (DTT) in cold acetone were added followed by placing the sample at −20 °C for 2 h to

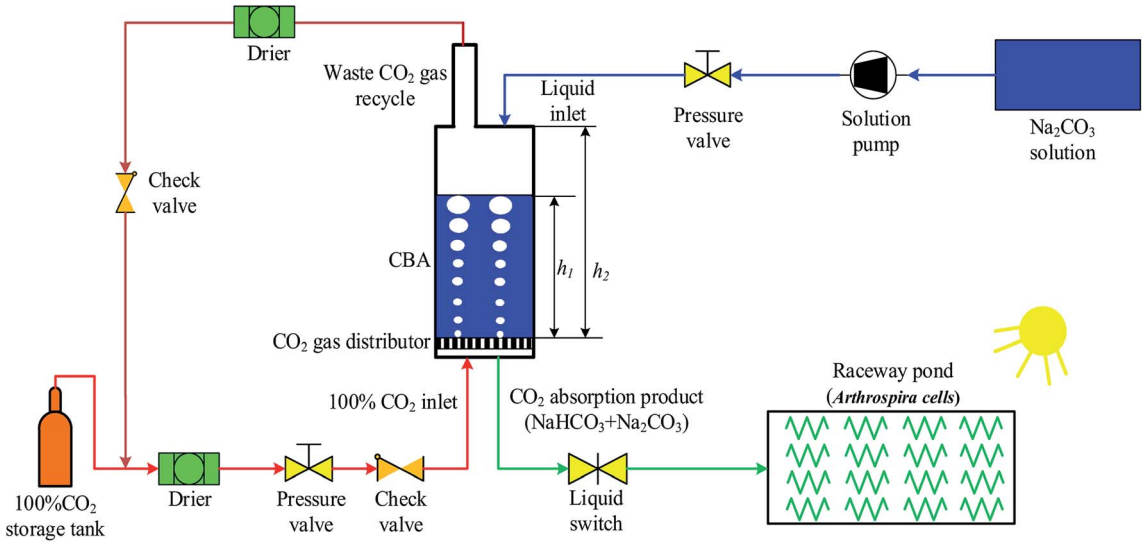

Fig. 1 Schematic diagram of an experimental system for a CO_2 bicarbonation absorber (CBA) for improving microalgal growth rate.

overnight for sample extraction. Samples were centrifuged and the pellet was washed twice with cold acetone. Finally, the pellet was resuspended in the dissolution buffer [Tris base (pH = 8) and 8 M urea].

2.3.2 Peptide preparation. The supernatant from each sample, containing precisely 0.1 mg of protein, DTT reduction and iodoacetamide alkylation, was digested using Trypsin Gold (Promega, Madison, WI, USA) at 37 °C for 16 h. After trypsin digestion, the peptide was desalted using a C_{18} cartridge to remove the high urea, and the desalted peptides were dried using vacuum centrifugation.

2.3.3 Liquid chromatography-mass spectrometry/mass spectrometry (LC-MS/MS) analysis. Each peptide sample was dissolved with loading buffer and then separated using a C_{18} column [75 μm inner diameter, 360 μm outer diameter × 10 cm, 1.9 μm C_{18}, (Dr Maisch HPLC GmbH)]. Mobile phase A consisted of 0.1% formic acid in water solution, and mobile phase B consisted of 0.1% formic acid in acetonitrile solution and a series of 60 min gradients were used which were adjusted according to the hydrophobicity of the fractions eluted in the one-dimensional (1D) LC with a flow rate of 300 nL min^{-1}. A Q-exactive HF-X hybrid quadrupole-Orbitrap MS (ThermoFisher) was operated in positive polarity mode with a capillary temperature of 320 °C. Full MS scan resolution was set to 60 000 with an automatic gain control target value of 3×10^6 for a scan range of 350–1500 *m*/*z*. The proteins found were identified using the functional database of the KEGG Pathway.[38,39]

3. Results and discussion

3.1 Optimizing operation conditions of CO_2 bicarbonation absorber to improve the microalgal growth rate

3.1.1 Optimizing reaction time. Kantarci *et al.*[40,42] proposed, that the reaction time of Na_2CO_3 and CO_2 in CBA was important. This is because the CO_2 dissolution rate in the liquid solution is slow, so most of the CO_2 gas gathered on the top of the free space causing a low contact area. In an actual application, a shorter reaction time would increase the work efficiency. Therefore, optimizing the reaction time was essential for obtaining the correct HCO_3^- concentration. As shown in Fig. 2(a), with an increase of reaction time from 30 min to 150 min, the TIC and $NaHCO_3$ concentrations increased from 219 mM L^{-1} to 350 mM L^{-1}, and from 98 mM L^{-1} to 350 mM L^{-1}, respectively. The molar proportion of $NaHCO_3$ in TIC (ω) increased from 45% to 100% and the CO_2 absorption volume increased from 69 mM L^{-1} to 551 mM L^{-1}. Lin *et al.*[41] also proved that increasing the reaction time was beneficial for $NaHCO_3$ production. However, the Na_2CO_3 concentration, decreased from 121 mM L^{-1} to 0.4 mM L^{-1}. The microalgal biomass growth rate first increased from 0.21 g L^{-1} d^{-1} to 0.55 g L^{-1} d^{-1}, and subsequently decreased to 0.36 g L^{-1} d^{-1}. It was found that the reaction of CO_2 and Na_2CO_3 required enough reaction time to enhance the production of $NaHCO_3$. When the reaction time was 150 min, the Na_2CO_3 was completely converted to $NaHCO_3$. However, the solution pH was low at these conditions, which affected the active transport of $NaHCO_3$. The algal growth was also not ideal under these conditions.

As shown in Fig. 2(b) and (c), as the reaction time increased from 30 min to 150 min, the initial solution pH decreased continually from 10.14 to 9.19. The biomass density was increased at first and then decreased, which may be a result of the ω and pH differences. When the reaction time was 90 min, the ω was 91% and the initial pH was 9.73, which was suitable for the growth of the microalgal cells. With the growth of the microalgal cells, the solution $NaHCO_3$ in the RWP decreased gradually while the Na_2CO_3 concentration increased. The biomass density and pH value also increased gradually. The reaction time caused the difference in the initial $NaHCO_3$ level in the solution, which was critical for the carbon concentrating mechanism (CCM) of the algal cells. As is known, the OH^- ions were exhausted causing an increase of pH value. According to the CCM, the HCO_3^- passed through the plasma membrane *via* the translocator *HLA3* and *LC11*, followed by passage through the chloroplast envelope *via* the translocator *LciA* and then the

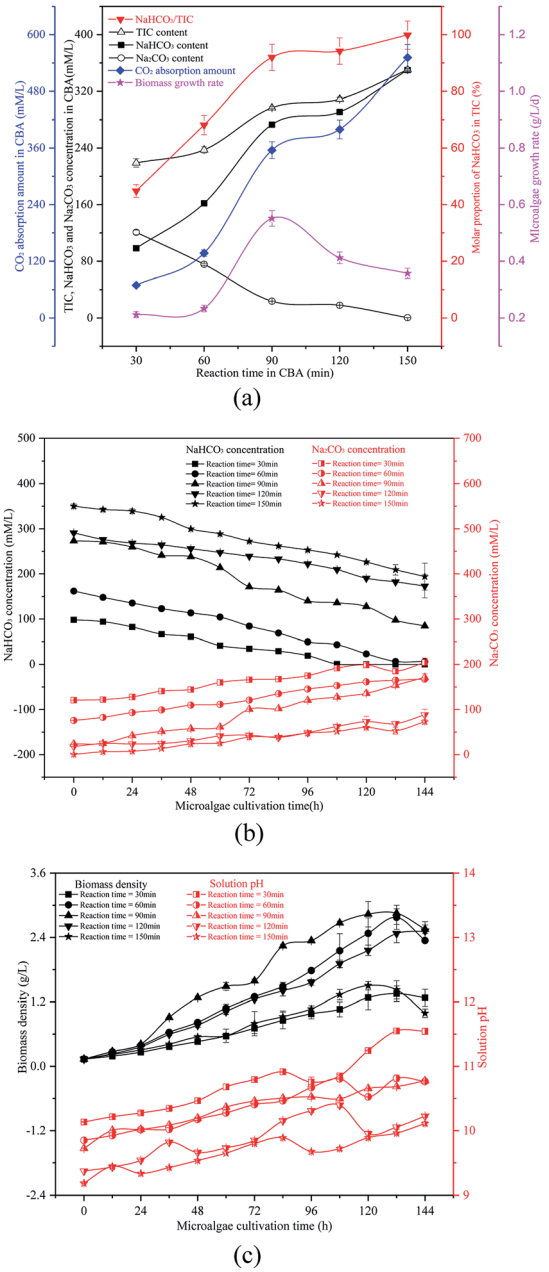

Fig. 2 Optimizing the reaction time in a CO_2 bicarbonation absorber (CBA) to regulate the production of the absorption product, $NaHCO_3$, (a) effects of reaction time, (b) dynamic changes of $NaHCO_3$ and Na_2CO_3 concentrations, and (c) biomass density and pH value.

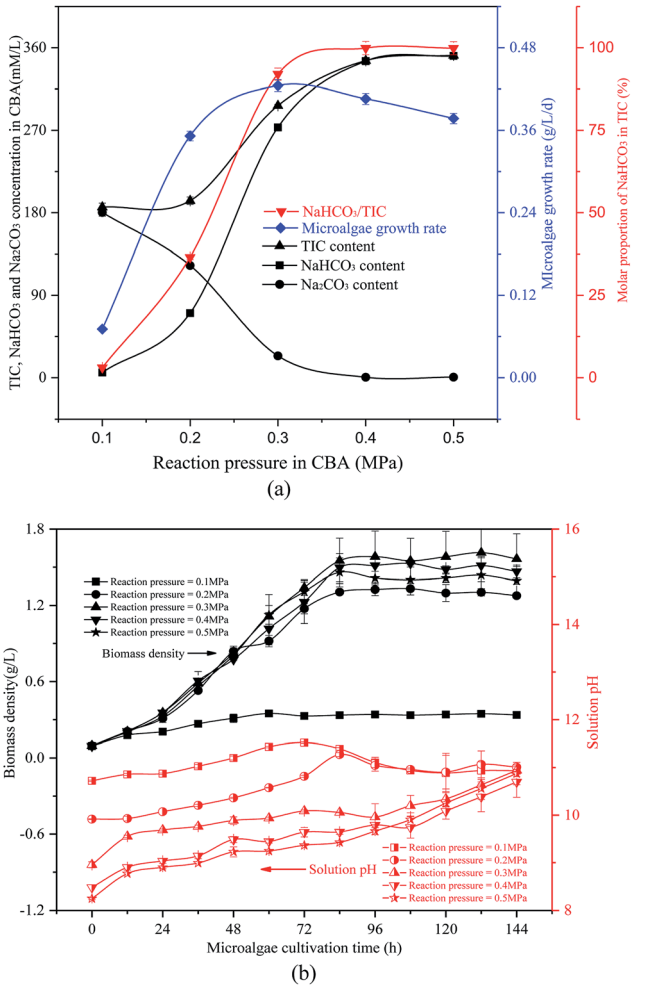

Fig. 3 Optimizing reaction pressure in a CO_2 bicarbonation absorber (CBA) to regulate the absorption of the product, $NaHCO_3$ (a) effects of reaction pressure, (b) biomass density and pH value.

thylakoid membrane *via* the translocator *LCI11*. The HCO_3^- finally reached the thylakoid lumen, where the HCO_3^- was catalysed to CO_2 by the *CAH3* enzyme. The CO_2 was fixed by the enzyme RuBisCO and was channelled into the Calvin cycle.[1,2] However, some of the HCO_3^- was catalysed by the CA in the periplasmic space and converted to CO_2, which was diffused to the stroma and captured by the RuBisCO.[1] The HCO_3^- was transported by the CA in cellular stroma during the growth of algal cells, so the HCO_3^- concentration decreased gradually while the CO_3^{2-} concentration increased. The HCO_3^- was the dominant carbon type to be absorbed by the algal cells. The presence of sufficient HCO_3^- promoted the Calvin cycle, and more adenosine triphosphate (ATP) was required, which in turn promoted photosynthesis to produce ATP. The HCO_3^- went through the cytoplasmic membrane by active transport, thereby enhancing the ion transport.

3.1.2 Optimizing reaction pressure. The reaction pressure was considered to be a key factor affecting the reaction of Na_2CO_3 and CO_2 in CBA.[42–44] As shown in Fig. 3(a), with the increase of reaction pressure from 0.1 MPa to 0.5 MPa in CBA, the TIC and $NaHCO_3$ concentration increased from 186 mM L^{-1} to 352 mM L^{-1} and from 5.7 mM L^{-1} to 351 mM L^{-1}, respectively. The ω increased continually from 3% to 99%; while the Na_2CO_3 concentration decreased from 180 mM L^{-1} to 0.6 mM L^{-1}. These results fully demonstrated that a higher reaction pressure promoted the production of $NaHCO_3$. According to the Gibbs free energy theory, the reaction of CO_2 and Na_2CO_3 was volume-reduced and was an exothermic reaction. The increase in pressure would promote the forward reaction, therefore the TIC and $NaHCO_3$ concentrations, as well as ω and the CO_2 absorption amount increased while the Na_2CO_3 decreased gradually. When the pressure was over 0.4 MPa, all the Na_2CO_3

was converted to $NaHCO_3$. These results were similar to those reported in other studies.[43,45,46]

The reacted $NaHCO_3$ and Na_2CO_3 mixtures were used to cultivate microalgal. Microalgal growth rate first increased from 0.07 g L^{-1} d^{-1} to 0.42 g L^{-1} d^{-1} and then decreased to 0.38 g L^{-1} d^{-1}. As shown in Fig. 3(b), with the growth of the algal cells, the biomass density and solution pH increased gradually. When the reaction pressure was 0.1 MPa, the microalgal nearly died, and the solution pH decreased slightly. That was because the solution $NaHCO_3$ concentration was pretty low under these conditions, which were not sufficient for photosynthesis in the microalgal. However, if the solution only consisted of $NaHCO_3$, the algal growth rate would also decrease. As the pH level was pretty low, it was not beneficial to the growth of the algal cells.

3.1.3 Optimizing initial sodium carbonate concentration. In the future it is hoped that it will be possible to produce more $NaHCO_3$ with less Na_2CO_3 substrate to reduce the economic costs of the process. Thus, the initial Na_2CO_3 concentration in CBA was studied. As shown in Fig. 4(a), with an increase in the initial Na_2CO_3 concentration from 120 mM L^{-1} to 280 mM L^{-1}, ω first increased from 88% to 92% and then decreased to 71%. The biomass growth rate first increased from 0.33 g L^{-1} d^{-1} to 0.45 g L^{-1} d^{-1} and then decreased to 0.29 g L^{-1} d^{-1}, and the $NaHCO_3$ concentration first increased from 203 mM L^{-1} to 273 mM L^{-1} and then decreased to 213 mM L^{-1}, whereas the CO_2 absorption amount decreased continually from 411 mM L^{-1} to 81 mM L^{-1}. The reason for this may be that with the initial Na_2CO_3 concentration increasing from 120 mM L^{-1} to 200 mM L^{-1}, the CO_2 gas and reaction time were sufficient, so more $NaHCO_3$ was produced, resulting in most of the Na_2CO_3 in the substrate being depleted, which was followed by an increase in ω. It seems that there was a saturation concentration of the $NaHCO_3$ and Na_2CO_3 mixture because with a further increase in substrate Na_2CO_3 concentration, it was more difficult for the reaction between Na_2CO_3 and CO_2 to occur. The ω and the concentration of the $NaHCO_3$ produced were decreased. It was noticed that the absorbed CO_2 concentration decreased continually. The reason for this may be that the accumulation rate of TIC decreased with an increase in substrate Na_2CO_3. The higher Na_2CO_3 concentration reduced the dissolution rate of CO_2, thus the CO_2 concentration decreased gradually. Furthermore, the biomass growth rate was increased first and then decreased, which was closely affected by the value of ω. As explained previously, the ω would promote the photosynthesis, and CO_2 fixation process. The accelerated Calvin cycle promoted the production of glyceraldehyde-3-phosphate (G3P), which was converted to carbohydrate. The carbohydrate caused an accumulation of biomass, thereby increasing the biomass growth rate.

The $NaHCO_3$ and Na_2CO_3 reaction mixtures were used to cultivate microalgal. Fig. 4(b) and (c) show the change in microalgal density and solution TIC. This demonstrated again that the optimized ω would promote microalgal growth. With the growth of the microalgal, the biomass density and solution pH increased gradually. In 0th, the order of the solution pH was $pH_{280\ mM\ L^{-1}} > pH_{240\ mM\ L^{-1}} > pH_{120\ mM\ L^{-1}} > pH_{200\ mM\ L^{-1}} = pH_{160\ mM\ L^{-1}}$. The reason behind this was that the solution pH

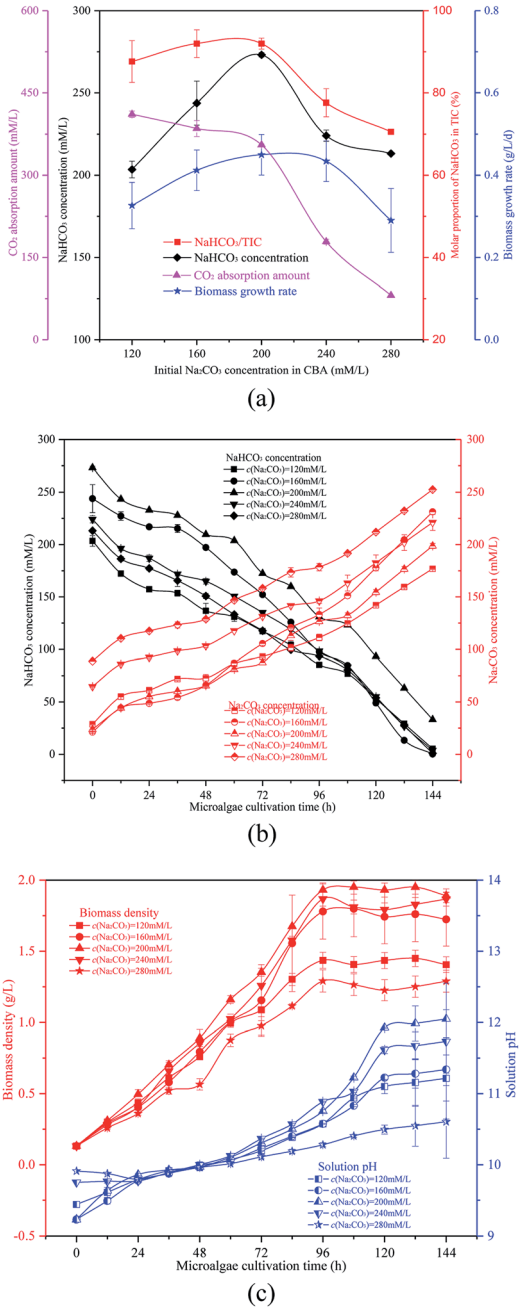

Fig. 4 Optimizing initial Na_2CO_3 concentration in the CO_2 bicarbonation absorber (CBA), (a) effects of initial Na_2CO_3 concentration, (b) dynamic changes of $NaHCO_3$ and Na_2CO_3 concentrations, and (c) biomass density and pH value.

was affected by ω which was different over the five different conditions. With the growth of algal cells, more OH^- were produced and more Na_2CO_3 was reacted. The order of biomass density was 200 mM L^{-1} > 240 mM L^{-1} > 160 mM L^{-1} > 120 mM L^{-1} > 280 mM L^{-1}. So the final solution pH also followed this order. Furthermore, the Na_2CO_3 concentration of the solution increased whereas the $NaHCO_3$ concentration decreased ($OH^- + HCO_3^- \rightarrow CO_3^{2-} + H_2O$), as shown in Fig. 4(c).

3.1.4 Optimizing the volume ratio of sodium carbonate solution. The influence of volume ratio of Na_2CO_3 solution (μ)

in the CBA on the production of $NaHCO_3$ was investigated further. As shown in Fig. 5(a), with an increase in the relative height of the solution from 20% to 100%, the TIC and $NaHCO_3$ concentrations decreased gradually from 311 mM L^{-1} to 179 mM L^{-1}, and from 310 mM L^{-1} to 59 mM L^{-1}, respectively. The ω and CO_2 absorption amount decreased from 100% to 33%, and from 408 mM L^{-1} to 0 mM L^{-1}, respectively, whereas the Na_2CO_3 concentration increased from 0.6 mM L^{-1} to 120 mM L^{-1}. The dissolution rate of the CO_2 gas was low and the reaction rate of CO_2 and Na_2CO_3 was slow. Thus, a space above the solution in the CBA was required for further reaction of CO_2. The gradual decrease of ω and CO_2 absorption amount proved this hypothesis. In a real application, it is essential to increase both the μ and ω to produce more $NaHCO_3$ in the mixture for large sale cultivation of microalgal.

The reacted solution mixture was used to cultivate the microalgal, and the biomass growth rate first increased from 0.27 g L^{-1} d^{-1} to 0.41 g L^{-1} d^{-1}, and then decreased to 0.28 g L^{-1} d^{-1}. As shown in Fig. 5(b), the biomass growth rate was dramatically higher when the μ in the CBA was 60% when compared with other conditions. When the μ was 100%, there was no CO_2 absorbed by the Na_2CO_3 solution, as there was no space above the solution. Therefore, almost no $NaHCO_3$ was produced under these conditions, however, sufficient $NaHCO_3$ is necessary for the growth of microalgae.

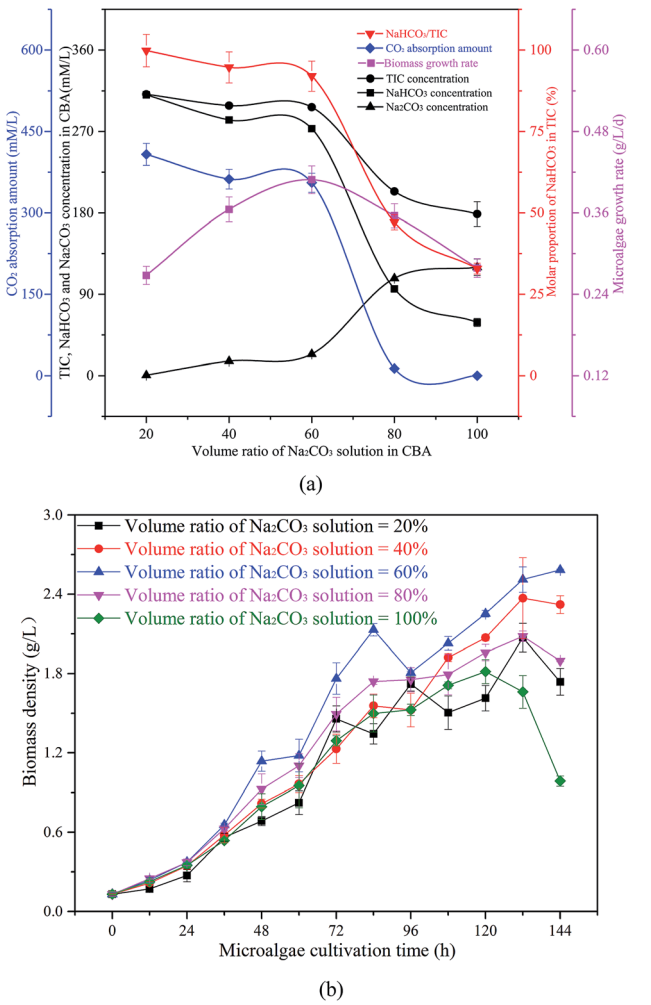

Fig. 5 Optimization of the volume ratio of Na_2CO_3 solution in the CO_2 bicarbonation absorber (CBA), (a) effects of volume ratio of Na_2CO_3 solution, (b) biomass density in microalgal growth.

3.2 Promoting the photosynthesis and carbon fixation metabolism pathway

It was noticed that the reaction pressure was essential for $NaHCO_3$ production, which further affects the biomass growth rate. The results in Fig. 3 show that the biomass growth rate under a CBA pressure of 0.3 MPa increased by 5.0 times compared with that obtained in 0.1 MPa. The ω was 92% when the reaction pressure was 0.3 MPa in CBA, which is ideal for the growth of algal cells. In order to investigate the molecular mechanism behind the improvement of microalgal growth rate under these conditions, label-free proteomics was conducted. The total number proteins identified in the *Arthrospira platensis* cells cultivated with the $NaHCO_3$ product converted from Na_2CO_3 solution at pressure of 0.1 MPa and 0.3 MPa, separately in the CBA was 1611. Meanwhile, the up-regulated protein number was 468 (29%), the down-regulated protein number was 541 (34%), and the insignificant-regulated protein number was 602 (37%).

As shown in Fig. 6(a), the enrichment pathway of the light reaction is shown along the electron transport chain. The light reaction of photosynthesis includes four stages: photosystem II (PSII), cytochrome b6/f complex (b6/f), photosystem I (PSI) and ATP synthase. The overall reaction formula is:

$$H_2O + ADP + Pi + [NADP] \rightarrow O_2 + ATP + NADPH + [H] \quad (1)$$

In the PSII stage, an H_2O molecule was disintegrated by the high light energy, and the H^+ proton gradient was established along the thylakoid membrane, and a high energy electron was released to the plastoquinone (Pq). This electron was transported to the b6/f, which also produced the H^+ proton and transferred it to the ATP synthase. The PSI reaction centre was P700, and the activated electron from P700 was transferred consecutively to the primary accepter (A_0), secondary acceptor (A_1), iron-sulfur protein and ferredoxin (F_d). The NADP reductase (FNR) then restored the $NADP^+$ to NADPH. At the same time, the H^+ produced in PSII and the b6/f was transferred to the ATP synthase, during which the phosphate ion (Pi) and ADP were consumed, and ATP was produced. As shown in Table 1, the D1 (*PsbA*) and D2 (*PsbD*) protein increased by 1.4 and 1.5 times, respectively. The PSII reaction centre proteins of CP43 (*PsbC*) and CP47 (*PsbB*) increased by 1.8 and 1.5 times, respectively. The PSI reaction centre (*PsaL* and *PsaE*) and iron-sulfur (*PsaC*) proteins increased by 96% and 93%, respectively. The PSI plastocyanin (*PsaF*) protein increased by 76%. The cytochrome proteins of b6 (*PetB*), f (*PetA*), ferredoxin (*PetF*) and c6 (*PetJ*) increased by 2.1, 1.4, 1.7 and 4.0 times, respectively. The ATP synthase subunit proteins of beta (*atpD*) and b (*atpF*) increased by 2.1 and 2.6 times, respectively, whereas the subunit a (*atpB*) decreased by 40%. The reason for this may be that the HCO_3^- concentration, at 0.3 MPa, of the CBA was

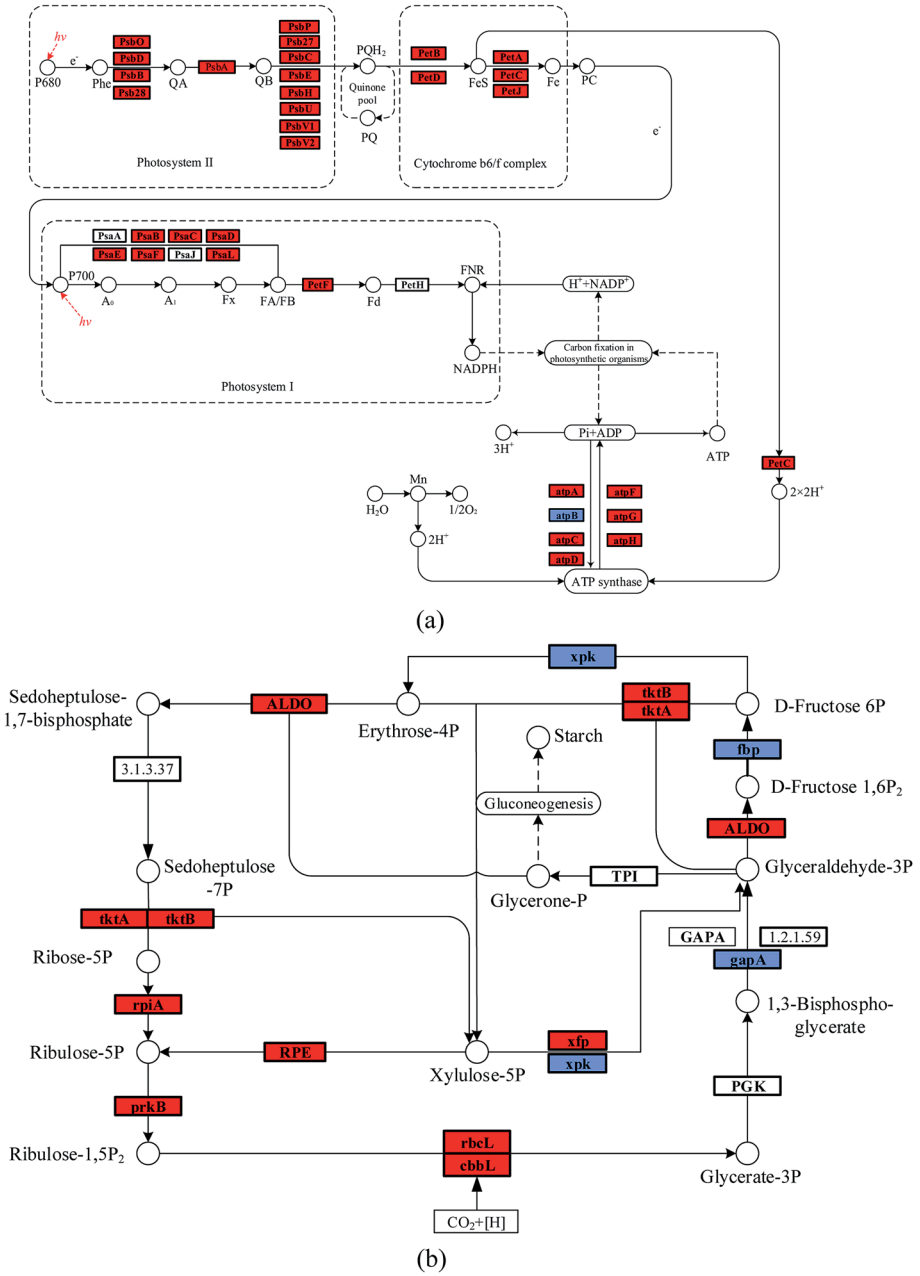

Fig. 6 Improved photosynthesis and carbon fixation pathways in *Arthrospira platensis* cells cultivated with the $NaHCO_3$ product at a pressure of 0.3 MPa in the CO_2 bicarbonation absorber, (a) improved photosynthesis pathway, (b) improved carbon fixation pathway (coloured boxes are *Arthrospira* specific enzymes, red boxes represent the up-regulated proteins, blue boxes represent the down-regulated proteins, and yellow boxes represent the uncertain-regulated proteins).

higher than that at 0.1 MPa, which was beneficial for the photosynthesis of the algal cells. As is known, the HCO_3^- ion can cross the cell membrane through active transportation, and was then catalysed to CO_2 by the inorganic carbon transporters (such as *LC11* and *HLA3*).[1,2] However, CA catalyses the extracellular HCO_3^- ion to CO_2, the CO_2 is diffused to the thylakoid membrane and fixed by the enzyme RuBisCO. Therefore, both of these methods required the participation of HCO_3^-. The higher HCO_3^- concentration required abundant ATP for the active transportation and dark reaction, the up-regulated ATP synthase subunit proteins of beta *atpD*, b *atpF*, and so on promoted the generation of ATP. In addition, the higher ATP consumption rate promoted the electron transport rate, thus, PSI and PSII were accelerated. The cytochrome complex, which was the electron carrier, was an essential protein in the electron transport chain. The up-regulated cytochrome proteins, such as b6 (*PetB*), f (*PetA*), ferredoxin (*PetF*) and c6 (*Petf*) also contributed to the light reaction. Once again, the higher HCO_3^- concentration promoted the generation of ATP, which was beneficial for the electron transport chain. The up-regulated cytochrome

Table 1 The significant expressed proteins of photosynthesis in *Arthrospira platensis* cells cultivated with the $NaHCO_3$ product in the CO_2 bicarbonation absorber. FC: fold change

Protein name	Gene	FC	log2FC	State
Photosystem II D1 protein	*PsbA*	2.42	1.28	Up
Photosystem II D2 protein	*PsbD*	2.45	1.29	Up
Photosystem II CP43 reaction centre protein	*PsbC*	2.75	1.46	Up
Photosystem II lipoprotein	*Psb27*	3.27	1.71	Up
Photosystem II CP47 reaction centre protein	*PsbB*	2.50	1.32	Up
Photosystem II CP47 reaction centre protein	*Psb28*	1.93	0.95	Up
Cytochrome b559 subunit alpha	*PsbE*	3.94	1.98	Up
Photosystem II reaction centre protein	*PsbH*	5.83	2.54	Up
Photosystem II 12 kDa extrinsic protein	*PsbU*	3.15	1.66	Up
Cytochrome c-550	*PsbV1*	2.21	1.14	Up
Photosystem II cytochrome	*PsbV2*	4.36	2.12	Up
Photosystem II manganese-stabilizing protein	*PsbO*	2.49	1.31	Up
Photosystem II oxygen evolving complex protein	*PsbP*	1.80	0.85	Up
Photosystem I P700 chlorophyll a apoprotein A2	*PsaB*	1.59	0.67	Up
Photosystem I iron-sulfur center	*PsaC*	1.93	0.95	Up
Photosystem I protein	*PsaD*	1.93	0.95	Up
Photosystem I reaction center subunit XI	*PsaL*	1.96	0.97	Up
Photosystem I reaction center subunit IV	*PsaE*	1.96	0.97	Up
Putative plastocyanin docking protein	*PsaF*	1.76	0.82	Up
Cytochrome b6	*PetB*	3.06	1.61	Up
Cytochrome b6-f complex subunit 4	*PetD*	3.00	1.58	Up
Cytochrome f	*PetA*	2.39	1.25	Up
Cytochrome b6-f complex iron-sulfur subunit	*PetC*	3.17	1.66	Up
Ferredoxin	*PetF*	2.66	1.41	Up
Cytochrome c6	*PetJ*	4.98	2.32	Up
ATP synthase subunit beta	*atpD*	3.14	1.65	Up
ATP synthase subunit alpha	*atpA*	1.91	0.93	Up
ATP synthase gamma chain gamma	*atpG*	2.36	1.24	Up
ATP synthase subunit delta	*atpH*	1.82	0.87	Up
ATP synthase epsilon chain epsilon	*atpC*	2.43	1.28	Up
ATP synthase subunit a	*atpB*	0.58	−0.79	Down
ATP synthase subunit b	*atpF*	3.57	1.84	Up

proteins and accelerated electron transport rate co-contributed to the reaction of PSI and PSII.

The enriched carbon fixation pathway is shown in Fig. 6(b). In the Calvin cycle, the CO_2 was catalysed by RuBisCO and was reacted with ribulose diphosphate (RuBP) to produce phosphoglycerate (PGA). The PGA reacted with ATP and NADPH to produce G3P that was transferred to carbohydrate and RuBP. The specific reaction formula is:

$$6CO_2 + 6RuBP + RuBisCO \rightarrow 12PGA \quad (2)$$

$$12PGA + 12ATP + 12NADPH + 6[H] \rightarrow 12\ G3P + 12[NADP] + 12Pi \quad (3)$$

$$2\ G3P \rightarrow (CH_2O) \quad (4)$$

$$10\ G3P + 6ATP \rightarrow 6RuBP + 6ADP + 4Pi \quad (5)$$

The higher HCO_3^- concentration mainly improved the expression of RuBisCO, as shown in Table 2, the RuBisCO (*rbcL*) and RuBisCO (*cbbL*) large chain increased by 3.5 and 2.4 times, respectively, improving the generation of G3P. The enzyme RuBisCO was important for the Calvin cycle, which determined the carbon assimilation rate of the photosynthesis. The up-regulated RuBisCO promoted the dark reaction of the algal cell, which accelerated the accumulation of biomass. In addition, the other proteins such as phosphoribulokinase (*prkB*), ribose-5-phosphate isomerase A (*rpiA*) and transketolase (*tktA*) were increased by 80%, 70% and 60%, respectively. These are helpful to the metabolism of pentose phosphate.

3.3 Practical applications of the CO_2 bicarbonation absorber and the raceway pond

The CBA-RWP has broad application prospects in engineering. The CO_2 gas added directly to the RWP caused a low CO_2 utilization efficiency. A huge amount of CO_2 gas was wasted and released to the atmosphere, causing secondary pollution. The $NaHCO_3$ was also used to cultivate the microalgal. However, the chemical $NaHCO_3$ was expensive. The price of *Spirulina* powder was around 1000–7000 $ per ton, whereas the $NaHCO_3$ was about 300–700 $ per ton with a consumption of 0.9–1.2 ton per ton algal powder, this accounted for a huge percentage of the operation costs. Combining CO_2 gas with Na_2CO_3 to cultivate microalgal has the potential to save on the operation costs and to reduce the CO_2 emission. Pure CO_2 gas was inexpensive, about 70–100 $ per ton. The Na_2CO_3 was 10–20 $ per ton and which can also be found in natural alkali lakes. During the later cultivation period, the Na_2CO_3 solution can be replaced by the

Table 2 The significant expressed proteins of carbon fixation in *Arthrospira platensis* cells cultivated with $NaHCO_3$ product in the CO_2 bicarbonation absorber

Protein name	Gene	FC	log2FC	State
Ribulose-bisphosphate carboxylase (RuBisCO)	*rbcL*	4.50	2.17	Up
Ribulose-phosphate 3-epimerase	*RPE*	4.09	2.03	Up
Fructose-bisphosphate aldolase class II	*ALDO*	3.65	1.87	Up
RuBisCO large chain	*cbbL*	3.35	1.74	Up
Transketolase domain protein	*tktB*	2.98	1.57	Up
D-fructose 6-phosphate phosphoketolase	*xfp*	2.16	1.11	Up
Phosphoribulokinase	*prkB*	1.80	0.85	Up
Ribose-5-phosphate isomerase A	*rpiA*	1.68	0.74	Up
Transketolase	*tktA*	1.59	0.67	Up
Glyceraldehyde-3-phosphate dehydrogenase	*gapA*	0.67	−0.59	Down
Probable phosphoketolase	*xpk*	0.63	−0.67	Down
Fructose-1,6-bisphosphatase class 1	*fbp*	0.50	−0.99	Down

wasted algal solution, as it contained a high sodium carbonate concentration. Also, the algal cell efficiently fixed CO_2 gas without any secondary pollution. Therefore, optimizing the CBA-RWP to cultivate microalgal was both economically and environmentally friendly.

4. Conclusions

A CO_2 bicarbonation absorber was proposed to efficiently convert CO_2 gas and Na_2CO_3 solution to produce $NaHCO_3$, which was easier to dissolve and remained for a longer time in the culture medium for promoting the microalgal growth rate. The CO_2 gas reacted with the Na_2CO_3 solution (initial concentration = 200 mM L^{-1} and the volume ratio in the CBA = 60%) for 90 min at 0.3 MPa to give the optimized molar proportion (92%) of the $NaHCO_3$ product in total inorganic carbon to increase the microalgal growth rate by 5.0 times. Expression levels of the PSII reaction centre protein (*PsbH*) and PSII cytochrome (*PsbV2*) in the photosynthesis pathway increased by 4.8 and 3.4 times, respectively, whereas that of the RuBisCO enzyme (*rbcL*) in the carbon fixation pathway increased by 3.5 times in *Arthrospira platensis* cells cultivated with the $NaHCO_3$ product at 0.3 MPa in the CBA. However, development of continuous flow is needed for the $NaHCO_3$ product, which would greatly improve the transfer efficiency, and would then be applicable for large-scale cultivation.

Conflicts of interest

There are no conflicts to declare.

Acknowledgements

This study was supported by the National Key Research and Development Program – China (2016YFB0601005), National Natural Science Foundation – China (51476141) and 2018 Zhejiang University Academic Award for Outstanding Doctoral Candidates.

References

1 L. C. M. Mackinder, C. Chen, R. D. Leib, W. Patena, S. R. Blum, M. Rodman, S. Ramundo, C. M. Adams and M. C. Jonikas, *Cell*, 2017, **171**, 133–147.
2 E. S. Freeman Rosenzweig, B. Xu, C. L. Kuhn, A. Martinez-Sanchez, M. Schaffer, M. Strauss, H. N. Cartwright, P. Ronceray, J. M. Plitzko and F. Förster, *Cell*, 2017, **171**, 148–162.
3 M. Giordano, J. Beardall and J. A. Raven, *Annu. Rev. Plant Biol.*, 2005, **56**, 99–131.
4 M. R. Badger, *J. Exp. Bot.*, 2003, **54**, 609–622.
5 J. Cabello, M. Morales and S. Revah, *Sci. Total Environ.*, 2017, **584–585**, 1310–1316.
6 J. Cheng, Z. Yang, Y. Huang, L. Huang, L. Hu, D. Xu, J. Zhou and K. Cen, *Bioresour. Technol.*, 2015, **190**, 235–241.
7 A. Janoska, P. P. Lamers, A. Hamhuis, Y. van Eimeren, R. H. Wijffels and M. Janssen, *Chem. Eng. J.*, 2017, **313**, 1206–1214.
8 A. Concas, M. Pisu and G. Cao, *Chem. Eng. J.*, 2010, **157**, 297–303.
9 C. Ji, J. Wang, R. Li and T. Liu, *Bioprocess Biosyst. Eng.*, 2017, **40**, 1079–1090.
10 V. Tesař, C. Hung and W. B. Zimmerman, *Sens. Actuators, A*, 2006, **125**, 159–169.
11 Z. Yang, J. Cheng, R. Lin, J. Zhou and K. Cen, *Bioresour. Technol.*, 2016, **211**, 429–434.
12 Y. Huang, S. Zhao, Y. Ding, Q. Liao, Y. Huang and X. Zhu, *Bioresour. Technol.*, 2017, **233**, 84–91.
13 J. Cheng, W. Guo, C. Cai, Q. Ye and J. Zhou, *Bioresour. Technol.*, 2017, **249**, 212–218.
14 Q. Zhang, S. Xue, C. Yan, X. Wu, S. Wen and W. Cong, *Bioresour. Technol.*, 2015, **198**, 150–156.
15 J. Cheng, Z. Yang, Q. Ye, J. Zhou and K. Cen, *Bioresour. Technol.*, 2015, **190**, 29–35.
16 Z. Chen, X. Zhang, Z. Jiang, X. Chen, H. He and X. Zhang, *Bioresour. Technol.*, 2016, **219**, 387–391.
17 C. U. Ugwu, H. Aoyagi and H. Uchiyama, *Bioresour. Technol.*, 2008, **99**, 4021–4028.
18 R. N. Singh and S. Sharma, *Renewable Sustainable Energy Rev.*, 2012, **16**, 2347–2353.

19 A. Behkish, R. Lemoine, R. Oukaci and B. I. Morsi, *Chem. Eng. J.*, 2006, **115**, 157–171.
20 A. V. Kulkarni and J. B. Joshi, *Chem. Eng. Res. Des.*, 2011, **89**, 1972–1985.
21 J. Cheng, J. Xu, H. Lu, Q. Ye, J. Liu and J. Zhou, *Bioresour. Technol.*, 2018, **261**, 151–157.
22 Z. Yang, J. Cheng, Q. Ye, J. Liu, J. Zhou and K. Cen, *Bioresour. Technol.*, 2016, **220**, 352–359.
23 D. G. Maharloo, A. Darvishi, R. Davand, M. Saidi and M. R. Rahimpour, *J. CO2 Util.*, 2017, **20**, 318–327.
24 B. Haut, V. Halloin, T. Cartage and A. Cockx, *Chem. Eng. Sci.*, 2004, **59**, 5687–5694.
25 N. Kantarci and B. K. O. Ulgen, *Cheminform*, 2005, **36**, 2263–2283.
26 R. S. Goharrizi and B. Abolpour, *Res. Chem. Intermed.*, 2013, **41**, 1459–1471.
27 C. Zhang, W. Li, Y. Shi, Y. Li, J. Huang and H. Li, *Bioresour. Technol.*, 2016, **209**, 351–359.
28 A. C. Eloka-Eboka and F. L. Inambao, *Appl. Energy*, 2017, **195**, 1100–1111.
29 K. Mokashi, V. Shetty, S. A. George and G. Sibi, *Achievements in the Life Sciences*, 2016, **10**, 111–117.
30 J. Cheng, H. Lu, H. Xin, W. Yang, J. Zhou and K. Cen, *Bioresour. Technol.*, 2017, **238**, 650–656.
31 R. Putt, M. Singh, S. Chinnasamy and K. C. Das, *Bioresour. Technol.*, 2011, **102**, 3240–3245.
32 O. Couvert, S. Guégan, B. Hézard, V. Huchet, A. Lintz, D. Thuault and V. Stahl, *Food Microbiol.*, 2017, **68**, 89–96.
33 C. Ji, J. Wang, R. Li and T. Liu, *Bioprocess Biosyst. Eng.*, 2017, **40**, 1079–1090.
34 J. Cheng, W. Guo, Y. Song, S. Kumar, K. Ameer Ali and J. Zhou, *Bioresour. Technol.*, 2018, **269**, 1–8.
35 L. J. Goeminne, K. Gevaert and L. Clement, *J. Proteomics*, 2017, **171**, 23–26.
36 J. Wu, Y. An, H. Pu, Y. Shan, X. Ren, M. An, Q. Wang, S. Wei and J. Ji, *Anal. Biochem.*, 2010, **398**, 34–44.
37 J. Wu, X. Xie, Y. Liu, J. He, R. Benitez, R. J. Buckanovich and D. M. Lubman, *J. Proteome Res.*, 2012, **11**, 4541–4552.
38 M. Kanehisa, S. Goto, S. Kawashima, Y. Okuno and M. Hattori, *Nucleic Acids Res.*, 2003, **32**, 277–280.
39 M. Kanehisa, S. Goto, M. Hattori, K. F. Aokikinoshita, M. Itoh, S. Kawashima, T. Katayama, M. Araki and M. Hirakawa, *Nucleic Acids Res.*, 2006, **34**, 354–357.
40 N. Kantarci and B. K. O. Ulgen, *Cheminform*, 2005, **40**, 2263–2283.
41 T. J. Lin, K. Tsuchiya and L. S. Fan, *AIChE J.*, 2010, **44**, 545–560.
42 N. Kantarci, F. Borak and K. O. Ulgen, *Process Biochem.*, 2005, **40**, 2263–2283.
43 P. M. Wilkinson, A. P. Spek and L. L. V. Dierendonck, *AIChE J.*, 1992, **38**, 544–554.
44 A. Behkish, R. Lemoine, R. Oukaci and B. I. Morsi, *Chem. Eng. J.*, 2006, **115**, 157–171.
45 D. N. Miller, *Ind. Eng. Chem. Process Des. Dev.*, 1980, **19**, 371–377.
46 H. M. Letzel, J. C. Schouten, R. Krishna and C. M. V. D. Bleek, *Chem. Eng. Sci.*, 1999, **54**, 2237–2246.